Research Article

Real-Time Hovering Control of Unmanned Aerial Vehicles

Cuauhtémoc Acosta Lúa (ID),[1,2] **Claudia Carolina Vaca García** (ID),[1] **Stefano Di Gennaro** (ID),[2,3] **B. Castillo-Toledo** (ID),[2,4] **and María Eugenia Sánchez Morales** (ID)[1]

[1]*Technological Sciences Department, La Cienega University Center, University of Guadalajara, Av. Universidad 1115, Ocotlán, Jalisco CP 47820, Mexico*
[2]*Center of Excellence DEWS (Design Methodologies of Embedded Controllers, Wireless Interconnect and Systems-on-chip), University of L'Aquila, Via Vetoio, Loc. Coppito, L'Aquila 67100, Italy*
[3]*Department of Information Engineering, Computer Science and Mathematics, University of L'Aquila, Via Vetoio, Loc. Coppito, L'Aquila 67100, Italy*
[4]*Center for Research and Advanced Studies, Campus Guadalajara, Av. del Bosque 1145 Col. El Bajío, Zapopan CP 45019, Mexico*

Correspondence should be addressed to Cuauhtémoc Acosta Lúa; cuauhtemoc.acosta@cuci.udg.mx

In this paper, the design of a controller for the altitude and rotational dynamics is presented. In particular, the control problem is to maintain a desired altitude in a fixed position. The unmanned aerial vehicle dynamics are described by nonlinear equations, derived using the Newton–Euler approach. The control problem is solved imposing the stability of the error dynamics with respect to desired position and angular references. The performance and effectiveness of the proposed control are tested, first, via numerical simulations, using the Pixhawk Pilot Support Package simulator provided by Mathworks. Then, the controller is tested via a real-time implementation, using a quadrotor Aircraft F-450.

1. Introduction

Quadrotors have recently attracted the attention of many researchers due to their interesting applications. As a matter of fact, the potential applications of such devices are countless. Examples of such applications include searching and surveillance, monitoring, and rescuing tasks. From a methodological point of view, the interest relies on the fact that a quadrotor is a complex underactuated system with high nonlinearities and strong dynamical couplings. Furthermore, it is affected by aerodynamic disturbances, unmodeled dynamics, and parametric uncertainties. Therefore, the quadrotors represent an interesting testbed for testing new control techniques.

There are a large number of works dealing with quadrotors. As far as the mathematical model is concerned, in Bouabdallah et al. [1], Zeng and Zhao [2], and Nagaty et al. [3], a Newton–Euler model was presented. Furthermore, Magnussen et al. [4] and Valenti et al. [5] considered quaternions to describe the angular kinematics, whilst

Antonio-Toledo et al. [6] applied the Euler–Lagrange equations to obtain the whole quadrotor mathematical model. Regarding the control of quadrotors, many control techniques have been proposed. In Panomruttanarug et al. [7] and Pounds et al. [8], the linear quadratic regulator control and the proportional integral derivative control, respectively, were exploited to design a control law. However, these controllers ensure only local stability. In order to enlarge the basin of attraction, nonlinear control techniques have also been considered. Examples are sliding model control Luque–Vega et al. [9], backstepping Bouabdallah and Siegwart [10], and adaptive control Matouk et al. [11]. Moreover, a global fast dynamic terminal sliding mode control method was proposed for position and attitude tracking control in Xiong and Zhang [12]. An adaptive command filtered backstepping control law was designed for trajectory tracking in Choi and Ahn [13]. In Liu et al. [14], a robust adaptive attitude tracking control for a quadrotor with an unknown inertia matrix and bounded external disturbances was proposed. A command filtered

implementation of an adaptive backstepping was proposed in Dong et al. [15], and the stability of the closed loop system was proved via the Lyapunov direct method. Finally, in Islam et al. [16], an observer-based adaptive fuzzy backstepping controller was designed for trajectory tracking, in the case of a quadrotor undergoing wind gusts and with parametric uncertainties. All these aforementioned methods provide good dynamic performance and robust stability and are tested mainly considering numerical simulations.

The main contribution of this paper is the design of a controller for the attitude and altitude of a quadrotor helicopter. This controller has been designed using the backstepping technique and has been tested using numerical simulations and real-time experimentation. In particular, the focus of this paper is to obtain a controller ensuring hovering so that

(1) The reference attitude is zero for the Euler angles describing the quadrotor angular position

(2) The reference altitude is a constant value

The performance and effectiveness of the proposed controller has been first tested with numerical simulations using the Pixhawk Pilot Support Package (PSP). Then, the real-time implementation has been performed implementing the proposed controller on a real F-450 quadrotor equipped of a Pixhawk and tested under environmental perturbations.

The paper is organized as follows. Section 2 introduces the description and the mathematical model of the quadrotor. In Section 3, the control problem is solved. In Section 4, numerical simulations and real-time tests are provided to show the effectiveness of the proposed controller. Finally, some concluding remarks are commented in Section 5.

2. Mathematical Model

The quadrotor considered in this work consists of a rigid frame equipped with four rotors. The rotors generate the propeller force $F_i = b\omega_{p,i}^2$, proportional to the propeller angular velocity $\omega_{p,i}$, $i = 1, 2, 3, 4$. The propellers 1 and 3 rotate counterclockwise, and the propellers 2 and 4 rotate clockwise.

Denote $RC(O, e_1, e_2, e_3)$ and $R\Gamma(\Omega, \varepsilon_1, \varepsilon_2, \varepsilon_3)$ as the frames fixed with the Earth and the quadrotor, respectively, with Ω coincident with the center of mass of the quadrotor (see Figure 1). The quadrotor absolute position in RC is described by $p = (x, y, z)^T$, whereas its attitude is described by the Euler angles $\alpha = (\phi, \theta, \psi)^T$, where $\phi, \theta, \psi \in (-\pi/2n, q\pi h/2)$ are the pitch, roll, and yaw angles, respectively. The sequence 3–2–1 has been considered by Huges [17]. Moreover, $v = (v_1, v_2, v_3)^T$ and $\omega = (\omega_1, \omega_2, \omega_3)^T$ are the linear and angular velocities of the center of mass of the quadrotor, expressed in RC and in RΓ, respectively.

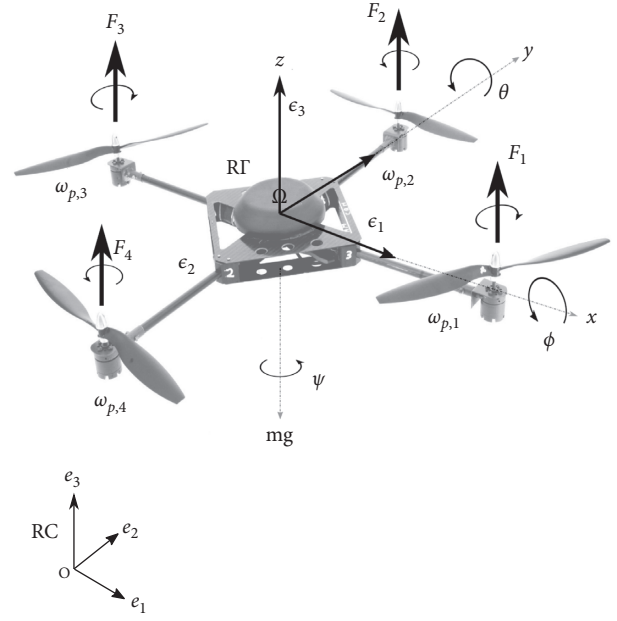The translation dynamics (in RC) and rotation dynamics (in the RΓ) of the quadrotor are

Figure 1: Quadrotor orientation using Euler angles.

$$\dot{p} = v,$$
$$\dot{v} = \frac{1}{m}\mathcal{R}(\alpha)F_{\text{prop}} + \frac{1}{m}F_{\text{grav}} + \frac{1}{m}F_d,$$
$$\dot{\alpha} = M(\alpha)\omega,$$
$$\dot{\omega} = J^{-1}\left(-\widetilde{\omega}J\omega + \tau_{\text{prop}} - \tau_{\text{gyro}} + M_d\right),$$

(1)

where m is the mass of the quadrotor, J is the inertia matrix of the quadrotor, and $J = \text{diag}\{J_x, J_y, J_z\}$ (expressed in RΓ), and

$$\widetilde{\omega} = \begin{pmatrix} 0 & -\omega_3 & \omega_2 \\ \omega_3 & 0 & -\omega_1 \\ -\omega_2 & \omega_1 & 0 \end{pmatrix},$$

(2)

is the so-called dyadic representation of ω,

$$F_{\text{prop}} = \begin{pmatrix} 0 \\ 0 \\ \sum_{i=1}^{4} F_i \end{pmatrix},$$

$$\tau_{\text{prop}} = \begin{pmatrix} \tau_1 \\ \tau_2 \\ \tau_3 \end{pmatrix} = \begin{pmatrix} l(F_2 - F_4) \\ l(F_3 - F_1) \\ c(F_1 - F_2 + F_3 - F_4) \end{pmatrix},$$

(3)

are the forces and moments produced by the propellers (inputs), with l as the distance between the center of mass to the rotor shaft. Moreover, $F_{\text{grav}} = (0 \ 0 \ -mg)^T$ is the force due to the gravity expressed in RC.

The vectors expressed in RΓ are transformed into vectors in RC by the rotation matrix:

$$\mathscr{R}(\alpha) = \begin{pmatrix} c_\theta c_\psi & s_\phi s_\theta c_\psi - c_\phi s_\psi & c_\phi s_\theta c_\psi + s_\phi s_\psi \\ c_\theta s_\psi & s_\phi s_\theta s_\psi + c_\phi c_\psi & c_\phi s_\theta s_\psi - s_\phi c_\psi \\ -s_\theta & s_\phi c_\theta & c_\phi c_\theta \end{pmatrix}, \quad (4)$$

with $c_\gamma = \cos(\gamma)$, $s_\gamma = \sin(\gamma)$, and $\gamma = \phi, \theta, \psi$. The angular velocity dynamics are expressed using the matrix:

$$M(\alpha) = \begin{pmatrix} 1 & s_\phi tg_\theta & c_\phi tg_\theta \\ 0 & c_\phi & -s_\phi \\ 0 & s_\phi sc_\theta & c_\phi sc_\theta \end{pmatrix}, \quad (5)$$

with $tg_\gamma = \tan(\gamma)$ and $sc_\gamma = \sec(\gamma)$.

The rolling torque τ_1 is produced by the forces F_2 and F_4. Similarly, the pitching torque τ_2 is produced by the forces F_1 and F_3. Due to Newton's third law, the propellers produce a yawing torque τ_3 on the body of the quadrotor, in the opposite direction of the propeller rotation. Moreover,

$$\tau_{\text{gyro}} = \sum_{i=1}^{4} (-1)^{i+1} J_p \omega_p \widetilde{\omega} \varepsilon_3, \quad (6)$$

is the gyroscopic torque due to the propeller rotations, with J_p the propeller moment of inertia with respect to its rotation axis. Finally, F_d and M_d are the forces and torques due to the external disturbances, which are assumed negligible here.

Under the assumption of small angles, matrix $M(\alpha)$ reduces to the identity matrix. This assumption is justified by the fact that the control objective is to maintain the quadrotor in an hover position Nagaty et al. [3]. This leads to a simplified mathematical model of the quadrotor given by

$$\ddot{x} = \frac{1}{m}\left(c_\phi s_\theta c_\psi + s_\phi s_\psi\right)u_1,$$

$$\ddot{y} = \frac{1}{m}\left(c_\phi s_\theta s_\psi - s_\phi c_\psi\right)u_1,$$

$$\ddot{z} = \frac{1}{m}c_\phi c_\theta u_1 - g,$$

$$\ddot{\phi} = \frac{J_y - J_z}{J_x}\dot{\theta}\dot{\psi} - \frac{J_p}{J_x}\omega_p\dot{\theta} + \frac{l}{J_x}\tau_1, \quad (7)$$

$$\ddot{\theta} = \frac{J_z - J_x}{J_y}\dot{\phi}\dot{\psi} + \frac{J_p}{J_y}\omega_p\dot{\phi} + \frac{l}{J_y}\tau_2,$$

$$\ddot{\psi} = \frac{J_x - J_y}{J_z}\dot{\phi}\dot{\theta} + \frac{1}{J_z}\tau_3,$$

where the control variables are defined as

$$u_1 = \sum_{i=1}^{4} F_i,$$

$$\tau_1 = l(F_2 - F_4), \quad (8)$$

$$\tau_2 = l(F_3 - F_1),$$

$$\tau_3 = c(F_1 + F_3 - F_2 - F_4),$$

where l is the distance of the center of mass to the rotor shaft, c is the drag factor, and $\omega_p = \omega_{p,1} - \omega_{p,2} + \omega_{p,3} - \omega_{p,4}$ is the so-called rotor relative speed. The parameters used in (7) and their values are defined in Table 1.

3. Control Design

3.1. Attitude Control. To design the attitude control law, let us define the following variables:

$$\phi = \phi_1,$$
$$\theta = \theta_1,$$
$$\psi = \psi_1,$$
$$\dot{\phi} = \phi_2, \quad (9)$$
$$\dot{\theta} = \theta_2,$$
$$\dot{\psi} = \psi_2,$$

so that system (7) can be rewritten as

$$\dot{\phi}_1 = \phi_2,$$

$$\dot{\phi}_2 = \frac{J_y - J_z}{J_x}\theta_2\psi_2 - \frac{J_p}{J_x}\omega_p\theta_2 + \frac{l}{J_x}\tau_1,$$

$$\dot{\theta}_1 = \theta_2,$$

$$\dot{\theta}_2 = \frac{J_z - J_x}{J_y}\phi_2\psi_2 + \frac{J_p}{J_y}\omega_p\phi_2 + \frac{l}{J_y}\tau_2, \quad (10)$$

$$\dot{\psi}_1 = \psi_2,$$

$$\dot{\psi}_2 = \frac{J_x - J_y}{J_z}\phi_2\theta_2 + \frac{1}{J_z}\tau_3,$$

where $X = (\phi_1, \phi_2, \theta_1, \theta_2, \psi_1, \psi_2)$ are the measured signals. The control objective is to match the UAV attitude X to a desired reference:

$$X_{\text{ref}} = \left(\phi_{1,\text{ref}}, \phi_{2,\text{ref}}, \theta_{1,\text{ref}}, \theta_{2,\text{ref}}, \psi_{1,\text{ref}}, \psi_{2,\text{ref}}\right). \quad (11)$$

To this aim, let us define the tracking errors as

$$e_{\phi,1} = \phi_1 - \phi_{1,\text{ref}},$$
$$e_{\phi,2} = \phi_2 - \phi_{2,\text{ref}} + k_1 e_{\phi,1},$$
$$e_{\theta,1} = \theta_1 - \theta_{1,\text{ref}},$$
$$e_{\theta,2} = \theta_2 - \theta_{2,\text{ref}} + k_3 e_{\theta,1}, \quad (12)$$
$$e_{\psi,1} = \psi_1 - \psi_{1,\text{ref}},$$
$$e_{\psi,2} = \psi_2 - \psi_{2,\text{ref}} + k_5 e_{\psi,1},$$

with $k_1, k_3, k_5 > 0$. Note that $e_{j,1} = 0$ implies $e_{j,2} = 0$, $j = \phi, \theta, \psi$. Deriving the error system (12) with respect to (10) is possible to calculate the error dynamics:

m	Mass of the airframe	1.1 kg
l	Distance of the center of mass to the rotor shaft	0.223 m
J_x	Inertia in the x-axis	6.825×10^{-3} kg m^2
J_y	Inertia in the y-axis	6.825×10^{-3} kg m^2
J_z	Inertia in the z-axis	12.39×10^{-3} kg m^2
J_p	Inertia of the propellers	6×10^{-5} kg m^2
g	Gravity acceleration	9.81 m/s^2
b	Thrust factor	54.2×10^{-6}
c	Drag factor	1.1×10^{-6} N s^2 rad^{-2}
ϕ	Roll angle	deg
θ	Pitch angle	deg
ψ	Yaw angle	deg
z_1	z-position	m

$$\dot{e}_{\phi,1} = e_{\phi,2} - k_1 e_{\phi,1} - \dot{\phi}_{1,\text{ref}} + \phi_{2,\text{ref}},$$

$$\dot{e}_{\phi,2} = \frac{J_y - J_z}{J_x}\theta_2\psi_2 - \frac{J_p}{J_x}\omega_p\theta_2 + \frac{l}{J_x}\tau_1,$$

$$- \dot{\phi}_{2,\text{ref}} + k_1\left(e_{\phi,2} - k_1 e_{\phi,1} + \phi_{2,\text{ref}} - \dot{\phi}_{1,\text{ref}}\right),$$

$$\dot{e}_{\theta,1} = e_{\theta,2} - k_3 e_{\theta,1} - \dot{\theta}_{1,\text{ref}} + \theta_{2,\text{ref}} = e_{\theta,2} - k_3 e_{\theta,1}$$

$$- \dot{\theta}_{1,\text{ref}} + \theta_{2,\text{ref}},$$

$$\dot{e}_{\theta,2} = \frac{J_z - J_x}{J_y}\phi_2\psi_2 + \frac{J_p}{J_y}\omega_p\phi_2 + \frac{l}{J_y}\tau_2,$$

$$- \dot{\theta}_{2,\text{ref}} + k_3\left(e_{\theta,2} - k_3 e_{\theta,1} + \theta_{2,\text{ref}} - \dot{\theta}_{1,\text{ref}}\right),$$

$$\dot{e}_{\psi,1} = e_{\psi,2} - k_5 e_{\psi,2} - \dot{\psi}_{1,\text{ref}} + \psi_{2,\text{ref}},$$

$$\dot{e}_{\psi,2} = \frac{J_x - J_y}{J_z}\phi_2\theta_2 + \frac{1}{J_z}\tau_3 - \dot{\psi}_{2,\text{ref}}$$

$$+ k_5\left(e_{\psi,2} - k_5 e_{\psi,1} + \psi_{2,\text{ref}} - \dot{\psi}_{1,\text{ref}}\right). \tag{13}$$

Using the following control law [18],

$$\tau_1 = \frac{J_x}{l}\left(-\frac{J_y - J_z}{J_x}\theta_2\psi_2 + \frac{J_p}{J_x}\omega_p\theta_2 + \dot{\phi}_{2,\text{ref}} - k_1\left(e_{\phi,2} - k_1 e_{\phi,1}\right.\right.$$

$$\left.\left. + \phi_{2,\text{ref}} - \dot{\phi}_{1,\text{ref}}\right) - k_2 e_{\phi,2}\right),$$

$$\tau_2 = \frac{J_y}{l}\left(-\frac{J_z - J_x}{J_y}\phi_2\psi_2 - \frac{J_p}{J_y}\omega_p\phi_2 + \dot{\theta}_{2,\text{ref}} - k_3\left(e_{\theta,2} - k_3 e_{\theta,1}\right.\right.$$

$$\left.\left. + \theta_{2,\text{ref}} - \dot{\theta}_{1,\text{ref}}\right) - k_4 e_{\theta,2}\right),$$

$$\tau_3 = J_z\left(-\frac{J_x - J_y}{J_z}\phi_2\theta_2 + \dot{\psi}_{2,\text{ref}} - k_5\left(e_{\psi,2} - k_5 e_{\psi,1} + \psi_{2,\text{ref}}\right.\right.$$

$$\left.\left. - \dot{\psi}_{1,\text{ref}}\right) - k_6 e_{\psi,2}\right), \tag{14}$$

with gains $k_i > 0$, $i = 2, 4, 6$ in (13), the tracking error dynamics become

$$\dot{e}_X = \begin{pmatrix} \dot{e}_{\phi,1} \\ \dot{e}_{\phi,2} \\ \dot{e}_{\theta,1} \\ \dot{e}_{\theta,2} \\ \dot{e}_{\psi,1} \\ \dot{e}_{\psi,2} \end{pmatrix} = \begin{pmatrix} -k_1 & 1 & 0 & 0 & 0 & 0 \\ 0 & -k_2 & 0 & 0 & 0 & 0 \\ 0 & 0 & -k_3 & 1 & 0 & 0 \\ 0 & 0 & 0 & -k_4 & 0 & 0 \\ 0 & 0 & 0 & 0 & -k_5 & 1 \\ 0 & 0 & 0 & 0 & 0 & -k_6 \end{pmatrix} \begin{pmatrix} e_{\phi_1} \\ e_{\phi_2} \\ e_{\theta_1} \\ e_{\theta_2} \\ e_{\psi_1} \\ e_{\psi_2} \end{pmatrix}$$

$$= A_X e_X, \tag{15}$$

where $e_X = \left(e_{\phi_1} \; e_{\phi_2} \; e_{\theta_1} \; e_{\theta_2} \; e_{\psi_1} \; e_{\psi_2}\right)^T$, which converge exponentially to zero. In fact, considering the Lyapunov candidate

$$V_X(t, e_X) = \frac{1}{2}e_X^T P_X e_X, \tag{16}$$

and differentiating along the error dynamics (15), one obtains

$$\dot{V}_X(t, e_X) = e_X^T\left(A_X^T P_X + P_X A_X\right)e_X = -e_X^T Q_X e_X$$

$$\leq -\lambda_{\min}^{Q_X}\|e_X\|^2 \leq -\alpha V_X(t, e_X), \quad \alpha = \frac{2\lambda_{\min}^{Q_X}}{\lambda_{\min}^{Q_X}} > 0, \tag{17}$$

with P_X solution of the equation $A_X^T P_X + P_X A_X = -Q_X$ for a fixed matrix $Q_X = Q_X^T > 0$. Therefore,

$$V_X(t, e_X) \leq e^{-\alpha t} V(0, e_X(0)), \tag{18}$$

so that the tracking error converges globally exponentially to zero [19].

3.2. Altitude Control.
For the altitude control, let us consider the altitude dynamics:

$$\dot{z}_1 = z_2,$$

$$\dot{z}_2 = g + c_{\phi_1}c_{\theta_1}\frac{1}{m}u_1. \tag{19}$$

The control problem is to maintain the quadrotor at a desired constant altitude $z_{1,\text{ref}}$, $z_{2,\text{ref}} = 0$. The tracking errors are defined as

$$e_{z,1} = z_1 - z_{1,\text{ref}},$$
$$e_{z,2} = z_2 - z_{2,\text{ref}}. \tag{20}$$

Choosing

$$u_1 = \frac{m}{c_{\phi_1} c_{\theta_1}} \left(g + \dot{z}_{2,\text{ref}} - k_{z,1} e_{z,1} - k_{z,2} e_{z,2} \right), \tag{21}$$

with $k_{z,1}, k_{z,2} > 0$, we obtain

$$\dot{e}_z = A_z e_z, \tag{22}$$

where $e_z = (e_{z,1}, e_{z,2})^T$ and

$$A_z = \begin{pmatrix} 0 & 1 \\ -k_{z,1} & -k_{z,2} \end{pmatrix}. \tag{23}$$

The stability proof is similar to that of the previous section.

4. Simulation and Experimental Results

In this section, the performance of the attitude and altitude controllers (14) and (21) is tested considering an F-450 quadrotor. First, numerical simulations are carried out. Then, real-time experimental tests are performed, showing the effectiveness of the control design.

4.1. Simulation Results.
For the numerical simulations, the quadrotor model provided by the Pixhawk PSP, in Simulink, has been used. This model contains the attitude and altitude flight control model called px4 demo attitude control, which shows a good performance in predicting the dynamic quadrotor behavior, very close to the real drone dynamics.

Controllers (14) and (21) use the nominal values of Table 1 and the gains of Table 2. The simulations have been performed in two steps. In the first one, the quadrotor is stabilized in altitude. In Figure 2, the altitude z is shown. In the second step, the quadrotor is stabilized in attitude. The pitch, roll, and yaw angles are shown in Figure 3. The initial conditions considered are $z(0) = 0$, $\phi(0) = -5.73°$, $\theta(0) = 5.73°$, and $\psi(0) = 5.73°$. The reference values are $z_{\text{ref}} = 2$ m and $\phi_{\text{ref}} = \theta_{\text{ref}} = \psi_{\text{ref}} = 0$.

4.2. Experimental Results.
In this section, we describe the physical setting of the embedded control that allows stabilizing the quadrotor. An embedded control system generally consists of three elements: sensors, actuators, and a microcontroller. The microcontroller interacts with the continuous dynamics of the plant via the sensors and actuators, and its major function is to compute and generate control commands for the actuators that are based on sensor measurements. The onboard electronic system consists of a flight controller, a hardware setup, and some ultrasonic sensors.

4.2.1. Flight Controller.
The 3DR-PIXHAWK is a high-performance autopilot-on-module suitable for fixed wing, multi rotors, helicopters, cars, boats, and other mobile robotic platforms. Its processor can run to 168 MHz/252 MIPS

TABLE 2: Gain values.

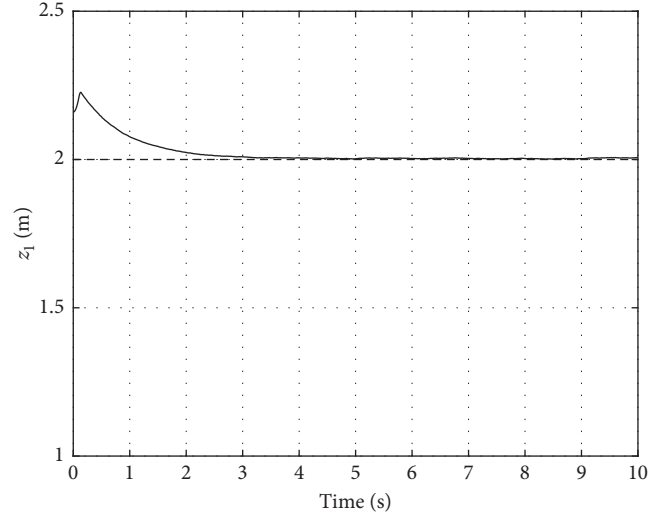| $k_{p,1} = 46$	$k_{d,1} = 35$	$k_{i,1} = 28$
$k_{p,2} = 4.3$	$k_{d,2} = 9$	$k_{i,2} = 0.2$
$k_{p,3} = 4.5$	$k_{d,3} = 7$	$k_{i,3} = 0.2$
$k_{p,4} = 7$	$k_{d,4} = 19$	$k_{i,4} = 0.1$

FIGURE 2: Numerical simulation: quadrotor's altitude z_1 (solid) and altitude reference $z_{1,\text{ref}}$ (dash).

Cortex-M4F with 256 KB in RAM and 2 MB flash and has 14 PWM/Servo outputs and abundant connectivity options for additional peripherals, such as 5x UART (serial ports), one high-power capable, 2x with HW flow control, 2x CAN, Spektrum DSM/DSM2/DSM–X® Satellite compatible input, PPM sum signal input, RSSI (PWM or voltage) input, I2C, SPI, 3.3 and 6.6 V ADC input. Moreover, the 3DR-Pixhawk has different sensors, such as ST Micro L3GD20H 16 bit gyroscopes, ST Micro LSM303D 14 bit accelerometers/magnetometers, Invensense MPU 6000 3-axis accelerometers/gyroscopes, and MEAS MS5611 barometers.

4.2.2. Hardware Setup.
The structure of the quadrotor is composed by an F-450 frame with integrated PCB wiring, whereas the rotors are brushless motors manufactured by E–max, with 935 rpm/V and a $10 \times 4.5''$ propellers. Turnigy speed drivers (ESC) are BHC type at 18 A max. The battery used in this setup is a 3S, 2800 mAh, 25C. The radio-transmitter is a Turnigy with 9 PPM channels working at 2.4 GHz.

An LV-MaxSonar-EZ4 sensor with a resolution of 2.54 cm, 20 Hz reading rate, 42 kHz ultrasonic sensor measures, a maximum Range of 645 cm, operating in the range of 2.5–5.5 VDC was used to measure the altitude.

For the real-time running, the same parameter values and gains shown in Table 2 were used. The initial condition for the altitude was $z(0) = 2.16$ m. For the pitch, roll, and yaw angles, the initial condition were chosen at $\phi_1(0) = 1.6°$, $\theta_1(0) = 0.9°$, and $\psi_1(0) = -1.6°$. Figures 4 and 5 show the dynamic behavior of the altitude and the pitch, roll, and yaw angles, respectively. It is worth noticing that these
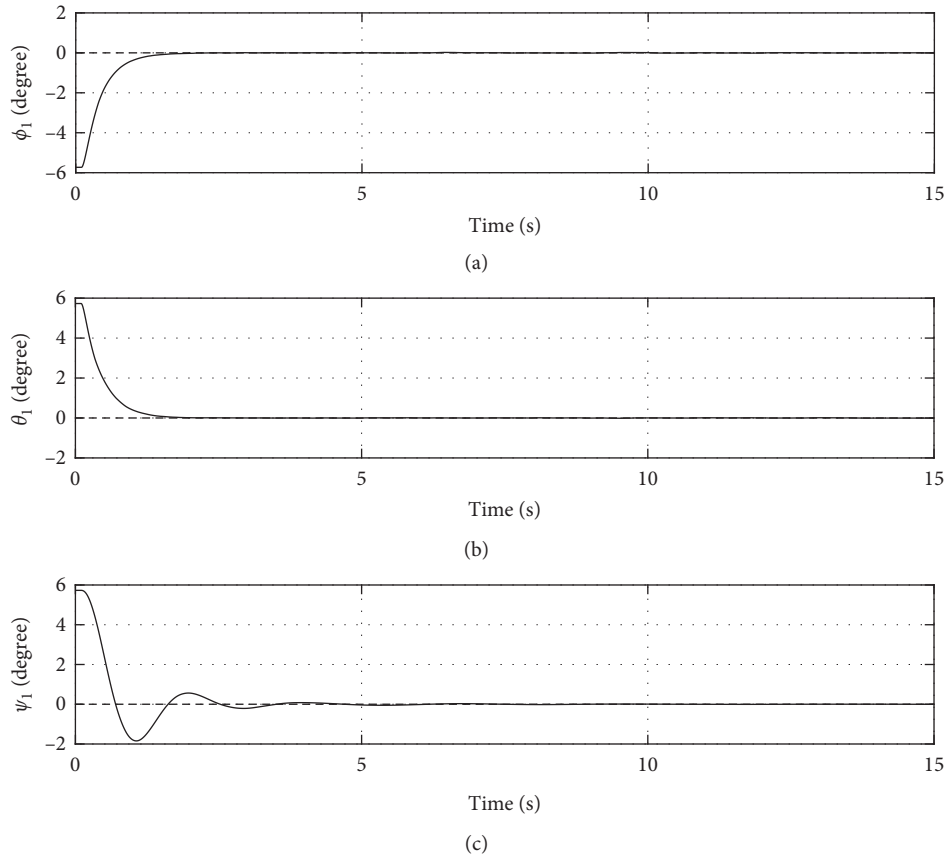
FIGURE 3: Numerical simulation: (a) roll angle ϕ_1 (solid) and roll angle reference $\phi_{1,\text{ref}}$ (dash); (b) pitch angle θ_1 (solid) and pitch angle reference $\theta_{1,\text{ref}}$ (dash); (c) yaw angle ψ_1 (solid) and yaw angle reference $\psi_{1,\text{ref}}$ (dash).
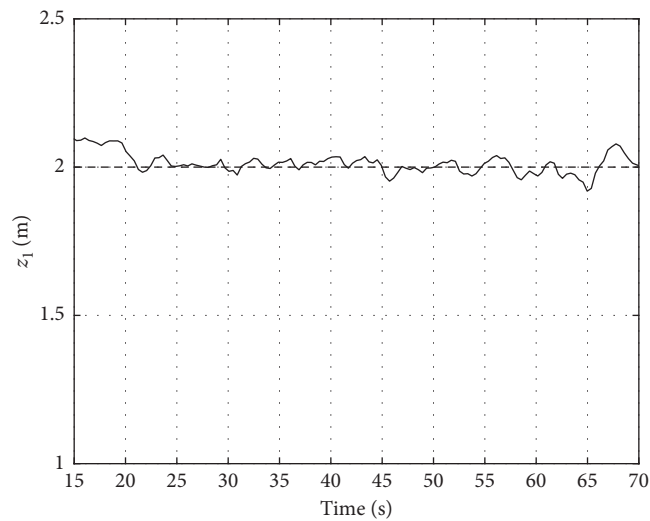

FIGURE 4: Experimental implementation: quadrotor's altitude z_1 (solid) and altitude reference $z_{1,\text{ref}}$ (dash).
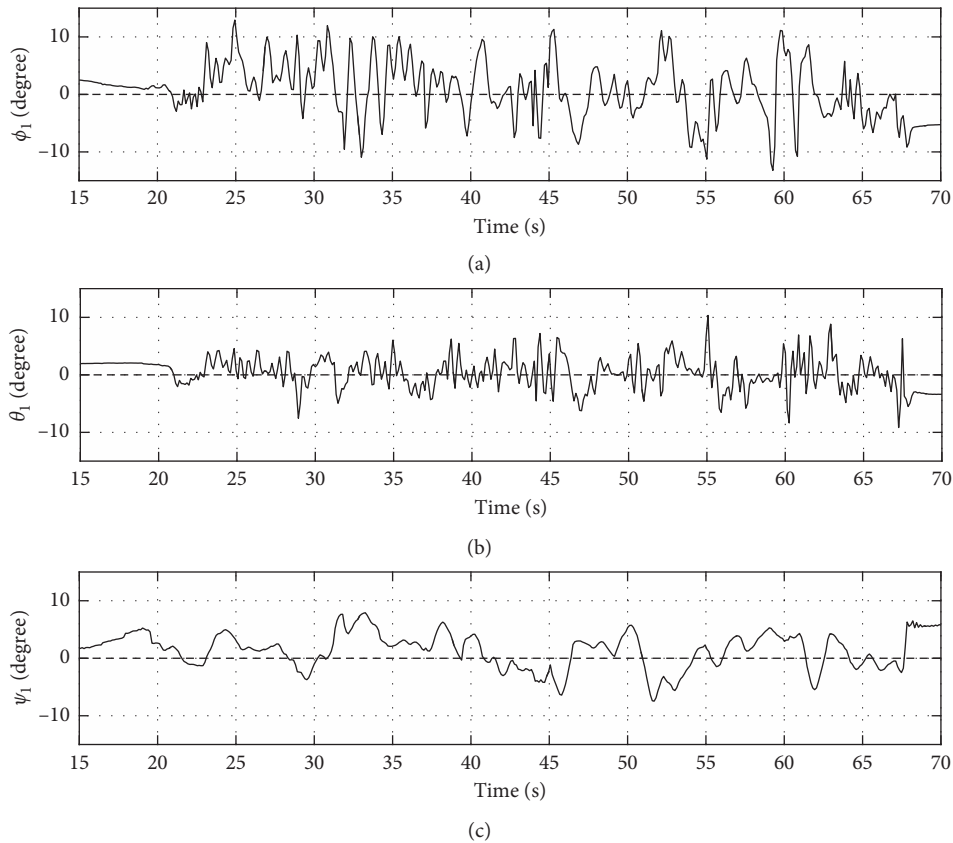
(a)

(b)

(c)

FIGURE 5: Experimental simulation: (a) roll angle ϕ_1 (solid) and roll angle reference $\phi_{1,\text{ref}}$ (dash) (degree vs. s); (b) pitch angle θ_1 (solid) and pitch angle reference $\theta_{1,\text{ref}}$ (dash) (degree vs. s); (c) yaw angle ψ_1 (solid) and yaw angle reference $\psi_{1,\text{ref}}$ (dash).

experimental tests were performed in an outdoor environment, without using the GPS sensor.

5. Conclusions

In this paper, a controller based on the stabilization technique for the altitude and attitude error has been proposed for a quadrotor. The simulation results have been performed using the Pixhawk PSP. Then, the controller has been implemented on a laboratory quadrotor. The simulation and experimental results show a good performance, even in outdoor environment, showing some degree of robustness in the presence of environmental disturbances.

Data Availability

The figures, tables, and other data used to support this study are included within the article.

Conflicts of Interest

The authors declare that there are no conflicts of interest regarding the publication of this paper.

Acknowledgments

References

[1] S. Bouabdallah, P. Murrieri, and R. Siegwart, "Design and control of an indoor Micro quadrotor," in *Proceedings of the IEEE International Conference on Robotics and Automation*, pp. 1–6, New Orleans, LA, USA, April-May 2004.

[2] Y. Zeng and L. Zhao, "Parameter identification for unmanned four–rotor helicopter with nonlinear model," in *Proceedings of the 2014 IEEE Chinese Guidance, Navigation and Control Conference,* pp. 922–926, Yantai, China, August 2014.

[3] A. Nagaty, S. Saeedi, C. Thibault, M. Seto, and H. Li, "Control and navigation framework for quadrotor helicopters," *Journal of Intelligent & Robotic Systems*, vol. 70, no. 1–4, pp. 1–12, 2013.

[4] O. Magnussen, M. Ottestad, and G. Hovland, "Experimental validation of a quaternion–based attitude estimation with direct input to a quadcopter control system," in *Proceedings of the International Conference on Unmanned Aircraft Systems (ICUAS)*, pp. 48–485, Atlanta, GA, USA, May 2013.

[5] R. Valenti, I. Dryanovski, and J. Xiao, "Keeping a good attitude: a quaternion-based orientation filter for IMUs and MARGs," *Sensors*, vol. 15, no. 8, pp. 19302–19330, 2015.

[6] M. Elena Antonio–Toledo, A. Y. Alanis, and E. N. Sanchez, "Robust neural decentralized control for a quadrotor UAV," in *Proceedings of the International Joint Conference on Neural Networks (IJCNN)*, pp. 714–719, Vancouver, Canada, July 2016.

[7] B. Panomruttanarug, K. Higuchi, and F. Mora-Camino, "Attitude control of a quadrotor aircraft using LQR state feedback controller with full order state observer," in *Proceeding of the International Conference on Instrumentation, Control and Information Technology (SICE)*, pp. 2041–2046, Konya, Turkey, June 2013.

[8] P. E. I. Pounds, D. R. Bersak, and A. M. Dollar, "Stability of small-scale UAV helicopters and quadrotors with added payload mass under PID control," *Autonomous Robots*, vol. 33, no. 1-2, pp. 129–142, 2012.

[9] L. Luque–Vega, B. Castillo–Toledo, and A. G. Loukianov, "Robust block second order sliding mode control for a quadrotor," *Journal of the Franklin Institute*, vol. 349, no. 2, pp. 719–739, 2012.

[10] S. Bouabdallah and R. Siegwart, "Backstepping and sliding-mode techniques applied to an indoor Micro quadrotor," in *Proceedings of the 2005 IEEE International Conference on Robotics and Automation*, Barcelona, Spain, April 2005.

[11] D. Matouk, O. Gherouat, F. Abdessemed, and A. Hassam, "Quadrotor position and attitude control via backstepping approach," in *Proceedings of the 8th International Conference on Modelling, Identification and Control (ICMI)*, pp. 73–79, Algiers, Algeria, November 2016.

[12] J.-J. Xiong and G.-B. Zhang, "Global fast dynamic terminal sliding mode control for a quadrotor UAV," *ISA Transactions*, vol. 66, pp. 233–240, 2017.

[13] Y. C. Choi and H. S. Ahn, "Nonlinear control of quadrotor for point tracking: actual implementation and experimental tests," *IEEE/ASME Transactions on Mechatronics*, vol. 20, no. 3, pp. 1179–1192, 2015.

[14] Y.-C. Liu, J. Zhang, T. Zhang, and J.-Y. Song, "Robust adaptive spacecraft attitude tracking control based on similar skew-symmetric structure," *Computers & Electrical Engineering*, vol. 56, pp. 784–794, 2016.

[15] W. Dong, J. A. Farrell, M. M. Polycarpou, V. Djapic, and M. Sharma, "Command filtered adaptive backstepping," *IEEE Transactions on Control Systems Technology*, vol. 20, no. 3, pp. 566–580, 2012.

[16] S. Islam, J. Dias, and L. D. Seneviratne, "Adaptive output feedback control for miniature unmanned aerial vehicle," in *Proceedings IEEE International Conference on Advanced Intelligent Mechatronics, AIM*, pp. 318–322, Banff, Canada, July 2016.

[17] P. C. Hughes, *Spacecraft Attitude Dynamics*, Dover Publications, Inc., Mineola, NY, USA, 1986.

[18] A. Isidori, *Nonlinear Control Systems*, Springer-Verlag, Berlin, Germany, 3rd edition, 1995.

[19] H. K. Khalil, *Nonlinear Systems*, Prentice-Hall, Upper Saddle River, NJ, USA, 2002.